N00014-76-C-0412

INTERACTION BETWEEN RANDOM WAVES AND HORIZONTAL SHEAR CURRENTS IN WATER OF VARYING DEPTH

By
Mehmet A. Tayfun
Robert A. Dalrymple
Cheng Y. Yang

Ocean Engineering Report No. 4

November 1975

Department of Civil Engineering
University of Delaware
Newark, Delaware

Geography Programs of the Office of Naval Research under contract No. N00014-76-C-0412

INTERACTION BETWEEN RANDOM WAVES AND HORIZONTAL SHEAR CHRRENTS IN WATER OF VARYING DEPTH

M. A. Tayfun, R. A. Dalrymple, C. Y. Yang

Department of Civil Engineering
University of Delaware
Newark, DE 19711

INTERACTION BETWEEN RANDOM WAVES AND HORIZONTAL SHEAR CURRENTS IN WATER OF VARYING DEPTH

Abstract

Interaction of incoherent random gravity waves with shear currents and underwater topography results in a spatial transformation of mean square spectral characteristics. For the particular case of unidirectional variations in currents and topography, this transformation involves a modification of spectral magnitudes and associated wave spaces in wave number or polar frequency-direction. Shear currents, in effect, act as a filter, dissipating and/or reflecting certain spectral components while transmitting others with substantial amplification or reduction in amplitude. These interactions are most noticeable in deep water and tend to be significantly diminished or modified in shallower depths by depth refraction and shoaling.

INTRODUCTION

Interaction between monochromatic waves and currents and/or underwater topography has been of considerable interest and usefulness in the study of waves and related phenomena in coastal waters. Munk and Traylor [1947] viewed wave refraction over an irregular topography as a primary mechanism controlling the spatial variation of wave characteristics which, in turn, becomes an important factor in various processes such as sediment transport, nearshore circulation and rip current generation. Similarly, Johnson [1947] and Arthur [1950] demonstrated the significant effects of the refraction of deep- and shallow-water waves encountering a current. Later, various investigators, e.g., Landau and Lifshitz [1959], Whitham [1960], Ursell [1960], Longuet-Higgins and Stewart [1961], Lighthill [1964], Bretherton and Garrett [1969], Dalrymple [1974 a,b], Peregrine [1975] and others, developed most of the systematic rules and concepts governing current-wave interactions. Explicit applications of these concepts to the computation of wave heights, wave kinematics and nearshore circulation are given by Kenyon [1971], Noda, et.al., [1974], Skovgaard, et.al., [1975], Dalrymple and Dean [1975].

It is, however, recognized that the description of the sea surface in terms of monochromatic waves is at best an approximation. Most realistic sea states have a more complex randomly irregular structure concisely characterized by a two-dimensional mean square spectral distribution over a wave number space or a polar frequency-direction space. Consequently, the extension of the concepts developed for the case of monochromatic waves interacting with currents and

underwater topography to the prediction of the spatial transformation of mean square spectral characteristics is a natural requirement. The earliest and most significant effort in this direction was made by Longuet-Higgins [1956, 1957], who considered the transformation of two-dimensional wave number spectra by refraction over a general underwater topography. Later, with the development of the radiation stress concept [Longuet-Higgins and Stewart, 1962], Phillips [1966] and Hasselmann [1968] generalized Longuet-Higgins' results and formulated a systematic energy approach for the prediction of spatially inhomogeneous spectra, taking into consideration current interactions, various dissipative and generative effects as well. The same approach has been recently extended to nonlinear random waves by Willebrand [1975]. However, explicit applications of this approach have been demonstrated only in a few cases. For example, Karlsson [1969] illustrated the refractive transformation of polar frequency-direction spectra over topographies with parallel and irregular bottom contours by numerical computation over a rectangular grid. Similarly, by also taking into account an approximate form of bottom friction, Collins [1972] developed a numerical ray tracing scheme to compute spatial variations in spectra due to refraction and shoaling. The refractive transformation of spectra over a topography with parallel bottom contours was further explored by Krasitskiy [1974]. In the case of unidirectional waves interacting with an opposing or following current in deep water, the explicit transformation for one-dimensional frequency spectra was given by Phillips [1966, p. 60]. The applications of this result to current measurements and wave forces were demonstrated by Huang et.al. [1972] and Tung and Huang [1973].

The motivation here is to study, via energy balance approach, the spatial transformation of spectral characteristics for directional random waves interacting with a steady nonuniform shear current in water of varying depth. In particular, the results obtained by Longuet-Higgins and Stewart [1961] for mono-

chromatic waves on a shearing current in deep water are generalized to include the case of random waves and the influence of one dimensional variations in underwater topography. It is, therefore, assumed that bottom contours are, in general, parallel to the current direction, restricting the spatial inhomogeneity of the problem to a single dimension. Emphasis is primarily placed on the spatial variation of two-dimensional spectral characteristics.

DEFINITIONS AND ANALYSIS

An incoherent random gravity wave field can be represented by

$$\eta(\underline{x},t) = \sum_n a_n(\underline{x},t) \cos \chi_n \tag{1}$$

where a_n is a Fourier amplitude regarded as a slowly varying function of time t and position $\underline{x} = (x_1, x_2)$ in a horizontal coordinate system fixed at still water level. The phase function

$$\chi_n(\underline{x},t) = \underline{k}_n \cdot \underline{x} - \omega_n t + \mu_n, \tag{2}$$

in which μ_n represents independent random phases uniformly distributed over $(0,2\pi)$, defines the vector wave number $\underline{k}_n$ and frequency ω_n in the usual way:

$$\underline{k}_n = \underline{\nabla}_2 \chi_n \quad , \quad \omega_n = -\partial\chi_n/\partial t \tag{3}$$

where $\underline{\nabla}_2 = (\partial/\partial x_1, \partial/\partial x_2)$ is the horizontal gradient operator.

It immediately follows from (3) that

$$\underset{2}{\nabla} \times \underline{k}_n = 0 \qquad \text{and} \qquad \frac{\partial \underline{k}_n}{\partial t} + \underset{2}{\nabla} \omega_n = 0 \tag{4}$$

are recognized, respectively, as the irrotationality condition and the kinematical conservation equation for the wave number $\underline{k}_n$.

Consider now the limiting case in which the vector wave numbers, $\underline{k}_n$, are distributed densely over a $\underline{k} = (k_1, k_2)$ plane. Correspondingly, the amplitudes a_n are such that if $(k_1, k_1 + dk_1; k_2, k_2 + dk_2)$ denotes any small region of the wave number plane then

$$\tfrac{1}{2}\sum_n^{d\underline{k}} a_n^2 = \psi(\underline{k}; \underline{x}, t)\, d\underline{k} \tag{4}$$

with $d\underline{k} = dk_1 dk_2$ as a shorthand notation and the sum is taken only over values of n for which $\underline{k}_n$ lies in the range $d\underline{k}$ around the fixed wave number $\underline{k}$. The spectral density, ψ, describes the distribution of the mean square surface deformation over $\underline{k}$-space locally, i.e.,

$$\langle |\eta(\underline{x}, t)|^2 \rangle = \tfrac{1}{2}\sum_n a_n^2 = \int_{\underline{k}} \psi(\underline{k}; \underline{x}, t)\, d\underline{k} \tag{5}$$

This distribution will be obviously different if the definition of wave space is changed. For instance, at any point $\underline{x}$ where ω and $\underline{k}$ are interrelated by a dispersion relation

$$\omega = \Omega(\underline{k}, \lambda) \tag{6}$$

in which the properties of the propagation medium are characterized by the function $\lambda(\underline{x}, t)$, we can write for the same mean square surface deformation

$$\langle |\eta(\underline{x},t)|^2 \rangle = \int_{\omega,\theta} \Phi(\omega,\theta;\underline{x},t)\ \omega\ d\omega\ d\theta \tag{7}$$

where θ, with $(k_1,k_2) = (k \cos\theta,\ k \sin\theta)$, is the direction of $\underline{k}$ relative to x_1 and the distribution Φ represents the so-called directional spectral density. ψ and Φ are connected by

$$\psi(\underline{k};\underline{x},t) = \frac{\omega}{k}\frac{\partial\Omega}{\partial k}\Phi(\omega,\theta;\underline{x},t) \tag{8}$$

so that

$$\psi\ d\underline{k} = \Phi\ \omega\ d\omega\ d\theta.$$

Consider now a medium with nonuniform still water depth $h(\underline{x},t)$ and moving with velocity $\underline{U}(\underline{x},z,t) = (U,V,W)$ relative to the fixed $(\underline{x},z)$ coordinate system. It is assumed that both h and $\underline{U}$ are slowly varying functions of time and space, and that the continuity equation for the mean flow is satisfied, i.e.,

$$\frac{\partial h}{\partial t} + \underline{U} \cdot \underline{\nabla}_3 h + h\ \underline{\nabla}_3 \cdot \underline{U} = 0 \tag{9}$$

where $\underline{\nabla}_3 = (\partial/\partial\underline{x},\ \partial/\partial z)$ is the three-dimensional gradient operator. We can write [Phillips, 1966, p. 43]

$$\omega = \Omega(\underline{k},\lambda) = \underline{U} \cdot \underline{k} + \omega' \tag{10}$$

where

$$\omega' = \Omega'(\underline{k},h) = [gk \tanh kh]^{1/2} \tag{11}$$

represents the frequency relative to a coordinate system moving with the current $\underline{U}$. Furthermore, the equations for wave rays are given as [see, e.g., Bretherton and Garrett, 1969; Kenyon, 1971]

$$\frac{d\underline{x}}{dt} = \frac{\partial \Omega}{\partial \underline{k}} \quad \text{and} \quad \frac{d\underline{k}}{dt} = -\frac{\partial \Omega}{\partial \lambda}\frac{\partial \lambda}{\partial \underline{x}} \tag{12}$$

Of the preceding expressions, the first describes a wave ray, i.e., the path traced out by an observer moving with the absolute group velocity

$$\underline{C}_G = \frac{\partial \Omega}{\partial \underline{k}} = \frac{\partial}{\partial \underline{k}}(\underline{U} \cdot \underline{k}) + \underline{C}'_G = (U + C'_G \cos\theta,\ V + C'_G \sin\theta) \tag{13}$$

in which

$$\underline{C}'_G = \frac{\partial \Omega'}{\partial k}\frac{\underline{k}}{k} = (C'_G \cos\theta,\ C'_G \sin\theta) \tag{14}$$

denotes the group velocity relative to $\underline{U}$, and the second equation describes the change in the vector wave number $\underline{k}$ along the ray. In this manner, we can define

$$\frac{d}{dt} = \frac{\partial}{\partial t} + \underline{C}_G \cdot \underline{\nabla}_2 \tag{15}$$

as differentiation moving with the group velocity $\underline{C}_G$.

The propagation of energy in a linear random wave field is described by an energy balance equation [Phillips, 1966, p. 147] derived under the general conditions of a medium with variable properties, nonuniform currents and various dissipation and generation effects. Under conservative conditions in which dissipation,

generation and wave-wave interactions can be neglected, the general form of the energy balance equation reduces, with a slight difference in notation, to

$$\rho g \left(\frac{\partial}{\partial t} + \underline{C}_G \cdot \underline{\nabla}_2\right) \psi + \frac{1}{2} S_{ij} \left(\frac{\partial U_i}{\partial x_j} + \frac{\partial U_j}{\partial x_i}\right) = 0 \tag{16}$$

where i,j = 1,2 refer to components associated with the horizontal coordinates x_1 and x_2 so that $U_1 = U$ and $U_2 = V$; S_{ij} denotes the spectral density of contributions to the radiation stress tensor given in the form

$$S_{ij} = \rho g\, n\, \psi(\underline{k};\underline{x},t) \left\{ \frac{k_i k_j}{k^2} + \left(1 - \frac{1}{2n}\right) \delta_{ij} \right\} \tag{17}$$

in which

$$n = \frac{C'_G}{C'} = \frac{1}{2} \left\{1 + \frac{2kh}{\sinh 2kh}\right\} \tag{18}$$

with

$$C' = \frac{\omega'}{k} \tag{19}$$

representing the relative phase speed, and $(k_1/k,\ k_2/k) = (\cos\theta,\ \sin\theta)$ are the components of the unit vector $\underline{k}/k$. Now, by exactly following the procedure described by Bretherton and Garrett [1969, p. 553] in the case of monochromatic waves, it can be shown that

$$\frac{1}{2} S_{ij} \left(\frac{\partial U_i}{\partial x_j} + \frac{\partial U_j}{\partial x_i}\right) = -\rho g \frac{\psi}{\omega'} \frac{d\omega'}{dt} \tag{20}$$

and, therefore, the energy balance equation (16) can be rewritten in a more concise, equivalent form as

$$\frac{d}{dt}\left(\frac{\psi}{\omega'}\right) = \left(\frac{\partial}{\partial t} + \underline{C}_G \cdot \underline{\nabla}_2\right)\left(\frac{\psi}{\omega'}\right) = 0 \tag{21}$$

It is evident that this equation describes the propagation of the quantity (ψ/ω'), referred to as wave action spectral density, in a general time dependent inhomogeneous medium, and it has been recently noted in a slightly different notation by Willebrand [1975], and previously by Bretherton and Garrett [1969] in a form applicable to monochromatic waves. Clearly (21) implies that

$$\frac{\psi}{\omega'} = \frac{\omega}{k}\frac{\partial \Omega}{\partial k}\frac{\phi}{\omega'} = \text{constant} \tag{22}$$

along a wave ray. Therefore, this result together with (12) and the initial values of ψ (or ϕ), $\underline{x}$ and $\underline{k}$ at one time are sufficient to determine the spectral density $\psi(\underline{k};\underline{x},t)$ or $\Phi(\omega,\theta;\underline{x},t)$. An obvious alternative that avoids the excessive numerical integration involved in ray tracing in general is to solve (21) by a finite difference approximation, this time, together with the irrotationality condition and the kinematical conservation equation (4) for the vector wave number $\underline{k}$.

In order to explore more explicitly what is involved in (22) in the following, we consider the simple yet interesting case of steady state conservative random waves propagating from a spatially homogeneous region such as deep water into an inhomogeneous region with a nonuniform depth profile $h(x)$, and traversing a steady nonuniform shear current, $\underline{U} = [0, V(x), 0]$. Hence, relative to a horizontal x,y-coordinate system fixed at still water level, the current direction and isobaths

are parallel to the y-axis, restricting the spatial inhomogeneity of the problem to the x-direction only. Under these conditions and from (4), the kinematical conservation law requires that the absolute frequency ω be invariant, i.e.,

$$\omega = \omega' + V(x)\, k \sin\theta = \text{constant} \tag{23}$$

where the angle θ relative to the x-axis is taken to be positive clockwise, and negative if counterclockwise. Similarly, the irrotationality condition on $\underline{k}$ implies that

$$k \sin\theta = \text{constant} \tag{24}$$

This is recognized as Snell's law. From (13) we have

$$\underline{C}_G = (C_G' \cos\theta,\ V(x) + C_G' \sin\theta) \tag{25}$$

Therefore, it is immediate from (21) or, simply from (22) that

$$\frac{\psi(\underline{k})}{[\omega - V(x)\, k \sin\theta]} = \frac{\omega}{k}\frac{\partial\Omega}{\partial k}\frac{\Phi(\omega,\theta)}{[\omega - V(x)\, k \sin\theta]} = \text{constant} \tag{26}$$

in the x-direction. It is understood in (26) that ψ and Φ are independent of time t, and the x-dependency of both quantities are kept implicit for convenience.

To specify various space-dependent quantities more explicitly, we will from now on designate deep water values that are spatially homogeneous in the absence of currents by the subscript (∞), those in finite nonuniform depth, h(x), in the absence of currents by the zero subscript, and leave all values in

the presence of a current unsubscripted irrespective of any depth consideration. In this manner, it can be shown first, from (11),(19),(23) and (24) that the function

$$\omega^2 \left[1 - \frac{V(x)}{C_\infty} \sin \theta_\infty\right]^2 = gk \tanh kh \tag{27}$$

represents the general dispersion relation, and

$$C = g\{\omega[1 - \frac{V(x)}{C_\infty} \sin \theta_\infty]\}^{-1} \tanh kh$$

$$= C_\infty \left[1 - \frac{V(x)}{C_\infty} \sin \theta_\infty\right]^{-1} \tanh kh \tag{28}$$

which is the phase speed relative to current, with the deep-water and finite-depth values in the absence of currents being given, respectively, by

$$C_\infty = \omega/k_\infty = g/\omega \tag{29}$$

$$C_o = \omega/k_o = C_\infty \tanh k_o h_o \tag{30}$$

Also, from (11), (23) and (27), we have

$$k = k_\infty \left[1 - \frac{V(x)}{C_\infty} \sin \theta_\infty\right]^2 (\tanh kh)^{-1} \tag{31}$$

and, on substitution from (24),

$$\sin \theta = (k_\infty/k) \sin \theta_\infty$$

$$= (\tanh kh) \left[1 - \frac{V(x)}{C_\infty} \sin \theta_\infty\right]^{-2} \sin \theta_\infty \tag{32}$$

Now, using (23) and the fact that $C_G' = \partial\omega'/\partial k = nC'$

$$\frac{\partial\Omega}{\partial k} = \underline{C}_G \cdot \frac{\underline{k}}{k} = C_G' + V(x) \sin\theta$$

$$= \frac{\omega}{k}\left[n + (1-n)\frac{V(x)}{C_\infty}\sin\theta_\infty\right] \tag{33}$$

with

$$\left(\frac{\partial\Omega}{\partial k}\right)_\infty = (C_G)_\infty = n_\infty \frac{\omega}{k_\infty} = \frac{1}{2}\frac{\omega}{k_\infty} \tag{34}$$

On the basis of the preceding definitions, it is observed that the simplest form of the constant in (26) is $\omega^{-1}\psi_\infty$ or $(C_\infty/2k_\infty)\Phi_\infty$. In terms of these and from (26) it follows, therefore, that the inhomogeneous densities $\psi(\underline{k})$ and $\Phi(\omega,\theta)$ are given by

$$\psi(\underline{k}) = \left[1 - \frac{V(x)}{C_\infty}\sin\theta_\infty\right]\psi_\infty(\underline{k}_\infty) \tag{35}$$

and

$$\Phi(\omega,\theta) = \frac{k\,C_\infty\left[1 - \frac{V(x)}{C_\infty}\sin\theta_\infty\right]}{2\,k_\infty\left[C_G' + V(x)\sin\theta\right]}\,\Phi_\infty(\omega,\theta_\infty) \tag{36}$$

CONSTRAINTS AND INTERPRETATION OF RESULTS

The general character of the preceding results indicates that the interaction between a random wave field and nonuniform current-depth effects involves a spatial transformation of the spectral magnitudes, ψ_∞, Φ_∞, and their respective

wave spaces. However, before we proceed to interpret this transformation, it is appropriate to discuss various kinematical and dynamical constraints embedded in the above equations. First, note from (35) and (36) that the condition

$$[1 - \frac{V(x)}{C_\infty} \sin \theta_\infty] \geq 0 \tag{37}$$

must be satisfied, in particular, by the components propagating in the direction of the current ($\theta_\infty > 0$). However, we also note from (32) that these components must locally have $\sin \theta \leq 1$, or equivalently

$$[1 - \frac{V(x)}{C_\infty} \sin \theta_\infty] \geq [(\tanh kh) \sin \theta_\infty]^{1/2} \tag{38}$$

Recognizing that $1 > \tanh kh \sin \theta_\infty > 0$, it is evident that the kinematical constraint implied by (38), only, is of any significance. At the lower limit when this constraint is an equality, $\sin \theta = \pi/2$ and the associated spectral component is totally reflected [Longuet-Higgins and Stewart, 1960].

It is noted, from (32), that the components with an initial angle of entry θ_∞ (or θ_o) < 0 will also have to have $\theta < 0$ locally. It follows, therefore, from (36), that these components must satisfy the condition

$$\frac{\partial \Omega}{\partial k} = [C_G' + V(x) \sin \theta] > 0 \tag{39}$$

In other words, the local relative group velocity, C_G', must be opposite in direction and larger in magnitude relative to the current velocity component, $V(x) \sin \theta$, in the direction of wave propagation. In the limit condition when

$C_G' = -V(x) \sin\theta$, the associated spectral component can no longer propagate against the current in that direction. Theoretically, the local spectral magnitude, Φ, becomes infinite, suggesting, therefore, that these spectral components will tend to diminish or attenuate by wave breaking and, possibly, by a lateral stretching in the crest direction before this point is reached. Note from (35) that the corresponding spectral magnitude, ψ, over $\underline{k}$-space remains always bounded (i.e., ≤ 2). It is, however, evident that (35) as well as all other results and definitions of the preceding analysis will lack validity near the critical point.

In summarizing the preceding discussion now, we may conclude that the spatial transformations of the spectral magnitudes, ψ_∞ and Φ_∞ via (35) and (36) are subject to the reflection constraint (38) for the components following the current ($\theta_\infty > 0$), and to the breaking constraint (39) for those opposing the current ($\theta_\infty < 0$). The latter can be rewritten, on substitution from (33) in terms of the homogeneous deep-water properties as

$$\frac{n}{(1-n)} \; C_\infty > -V(x) \sin\theta_\infty \qquad (40)$$

The transformations of the incident densities, Φ_∞ and ψ_∞ are, therefore, continuous in x for all but the attenuated and reflected components. The regions of the incident, $\underline{k}_\infty$- or ω,θ_∞-space that violate either of these constraints at a point are cut-off or, simply deleted at that point, assuming the absence of any sort of interaction between the attenuated and/or reflected components and those remaining. However, the original incident wave space is to be properly modified, as will be illustrated later with examples, by the reflected components in a manner consistent with the steady state assumption.

The spatial transformation of the magnitude ψ_∞ is entirely due to the current interaction in contrast with the transformation of Φ_∞ that involves the combined current-depth effects. The spectral magnitude ψ_∞ associated with the components at an opposing angle of incidence ($\theta_\infty < 0$) are amplified, and those with the current ($\theta_\infty > 0$) are reduced irrespective of any depth consideration. In the case of Φ_∞, the current effect on the spectral components with an opposing angle of entry is qualitatively the same as in the case of ψ_∞, i.e., amplification. However, for the components Φ_∞ following the current, the net effect of the combined current-depth interactions could be an amplitude amplification or reduction depending, respectively on whether a particular component is in shallow water or not. The spectral components ψ_∞ with the normal incidence ($\theta_\infty = 0°$) are entirely unaffected and remain spatially invariant; whereas for the same angle of incidence, Φ_∞ values may vary significantly due to wave shoaling represented by the term

$$\frac{k(C_G)_\infty}{k_\infty C'_G} = \frac{(C\ C_G)_\infty}{(C\ C_G)} \tag{41}$$

in (25). The local $\underline{k}$-space associated with the transformed magnitude ψ is distorted by the combined current-depth effects, obviously, in terms of the magnitude k as well as the direction θ of the wave number vector $\underline{k}$. As expected, the distortion by depth refraction is more pronounced in the range of small wave numbers while the current refraction in general affects the higher values. On the other hand, the distortion in the polar ω,θ-space is entirely due to the spatial dependence of θ. Since the complete spectral transformations require the mapping of the density ψ or Φ desirably in the form of contours in the local

wave space, the invariant nature of the frequency ω makes the polar ω,θ-space particularly advantageous to work with. Therefore, the discussion will be restricted to this space from now on.

COMMENTS ON SPATIAL VARIATION OF MEAN ENERGY

Mean total wave energy per unit horizontal area is defined by [Phillips, 1966, p. 27]

$$E = \rho g \langle |\eta|^2 \rangle = \rho g \int_{\omega,\theta} \Phi(\omega,\theta)\ \omega\ d\omega\ d\theta \tag{42}$$

In order to comment briefly on the spatial variation of this quantity for the particular case of interest here, it will be expedient to write

$$\Phi(\omega,\theta)\ \omega\ d\omega\ d\theta = \Phi(\omega,\theta)\ \omega\ d\omega \frac{\partial\theta}{\partial\theta_\infty}\ d\theta_\infty \tag{43}$$

where, by virtue of (32),

$$\frac{\partial\theta}{\partial\theta_\infty} = \frac{k_\infty}{k \cos\theta}\ \left(\cos\theta_\infty - \frac{\sin\theta_\infty}{k}\frac{\partial k}{\partial\theta_\infty}\right) \tag{44}$$

and, from (31),

$$\frac{\partial k}{\partial\theta_\infty} = -\frac{k\ k_\infty\ V(x) \cos\theta_\infty}{n\ \omega\left[1 - \frac{V(x)}{C_\infty}\sin\theta_\infty\right]} \tag{45}$$

On substitution from (44) and (45) we find that (43) becomes

$$\Phi(\omega,\theta)\ \omega\ d\omega\ d\theta = \frac{(n \sin 2\theta)_\infty}{n \sin 2\theta}\ \Phi_\infty(\omega,\theta_\infty)\ \omega\ d\omega\ d\theta_\infty \tag{46}$$

Therefore, (42) can be rewritten as

$$E = \rho g \int_{\omega,\theta_\infty\ \varepsilon\ R} \frac{(n \sin 2\theta)_\infty}{n \sin 2\theta}\ \Phi_\infty(\omega,\theta_\infty)\ \omega\ d\omega\ d\theta_\infty \tag{47}$$

where R represents the region of the incident ω,θ_∞-space that is not deleted by wave breaking and/or reflection as waves propagate to the point of interest. In deep water in the presence of currents (47) reduces to

$$E = \rho g \int_{\omega,\theta_\infty\ \varepsilon\ R} \frac{\sin 2\theta_\infty}{\sin 2\theta}\ \Phi_\infty(\omega,\theta_\infty)\ \omega\ d\omega\ d\theta_\infty \tag{48}$$

and, obviously, to the constant

$$E_\infty = \rho g \int_{\omega,\theta_\infty} \Phi_\infty(\omega,\theta_\infty)\ \omega\ d\omega\ d\theta_\infty \tag{49}$$

in the absence of any currents. Finally, at intermediate water depths in the absence of currents we find that (47) becomes

$$E_o = \rho g \int_{\omega,\theta_\infty} \frac{(C_G \cos\theta)_\infty}{(C_G \cos\theta)_o}\ \Phi_\infty(\omega,\theta_\infty)\ \omega\ d\omega\ d\theta_\infty \tag{50}$$

An examination of (47), (48) and (50) indicates that these definitions are, in fact, generalizations to various well-known results associated with monochromatic waves and, of course, with a narrow-band random wave field. In the case of monochromatic waves with the incident height H_∞, frequency ω, direction θ_∞, and energy

$$E_\infty = \rho g \int [(1/8)\ H_\infty^2\ \delta(\tilde{\omega} - \omega)\delta(\tilde{\theta}_\infty - \theta_\infty)]\ d\tilde{\omega}\ d\tilde{\theta}_\infty = (1/8)\rho g\ H_\infty^2 \tag{51}$$

we find

$$E = \frac{(n \sin 2\theta)_\infty}{n \sin 2\theta} E_\infty \tag{52}$$

$$E = \frac{\sin 2\theta_\infty}{\sin 2\theta} E_\infty \tag{53}$$

$$E_o = \frac{(C_G \cos\theta)_\infty}{(C_G \cos \theta)_o} E_\infty \tag{54}$$

corresponding to (47), (48) and (50), respectively. Of the preceding expressions, the last two have been previously given elsewhere [e.g., see Longuet-Higgins and Stewart, 1960; Phillips, 1966, p. 53]. The generalization of these results represented by the form (52) has not been observed before. It was informally suggested [e.g., see Longuet-Higgins, 1972] that (53), which is relevant only to deep water conditions, may be applicable to wave-current interactions at finite depth equally as well. It is evident now that this is not so.

ILLUSTRATIVE EXAMPLES

In order to illustrate the transformation of the directional spectral density $\Phi(\omega,\theta)$ more explicitly, it is worthwhile to examine some specific examples. For simplicity in presentation the examples will be confined to deep and shallow-water conditions where various key definitions involved in the transformation (36) become analytically tractable. Furthermore, it will be convenient to nondimensionalize various quantities in terms of the value $V_m = \max V(x)$ as follows:

$$\omega^* = (\omega\ V_m)/g \tag{55}$$

$$k^* = (k\ V_m^{\,2})/g \tag{56}$$

$$h^* = gh(x)/V_m^{\,2} \tag{57}$$

$$\Phi^*(\omega^*,\theta) = (g/V_m)^2\ \Phi(\omega,\theta) \tag{58}$$

so that

$$\Phi^*\omega^* d\omega^*\ d\theta = \Phi\ \omega\ d\omega\ d\theta \tag{59}$$

The explicit form of the incident spatially homogeneous deep water spectral density in both examples is assumed to be

$$\Phi_\infty^*\ (\omega^*,\theta_\infty) = \begin{cases} 1 \ ; & 1/2 \le \omega^* \le 3,\ |\theta_\infty| \le \pi/2 \\ 0 \ ; & \text{otherwise} \end{cases} \tag{60}$$

The incident ω^*,θ_∞-space has, therefore, a semi-annular shape as schematically illustrated in Figures 1 and 7.

Example 1: Current Interactions in Deep Water

In deep water, (32), (38), (40) and (36) become

$$\sin\theta = [1 - \frac{V(x)}{V_m}\omega^* \sin\theta_\infty]^{-2} \sin\theta_\infty \tag{61}$$

$$\frac{V(x)}{V_m}\omega^* \sin\theta_\infty \leq (1 - \sin^{1/2}\theta_\infty) \quad , \quad \theta_\infty > 0 \tag{62}$$

$$-\frac{V(x)}{V_m}\omega^* \sin\theta_\infty < 1 \quad , \quad \theta_\infty < 0 \tag{63}$$

$$\Phi^*(\omega^*,\theta)/\Phi^*_\infty(\omega^*,\theta_\infty) = A \tag{64}$$

where the spectral amplification factor, A is in the form

$$A = [1 - \frac{V(x)}{V_m}\omega^* \sin\theta_\infty]^5[1 + \frac{V(x)}{V_m}\omega^* \sin\theta_\infty]^{-1} \tag{65}$$

The shear current field, V(x), shown schematically in Figure 1, consists of regions of monotonic increase and decrease. It is evident from (65) and (61) that

$$A \begin{cases} > 1 \ (\theta_\infty < 0) \\ = 1 \ (\theta_\infty = 0) \\ < 1 \ (\theta_\infty > 0) \end{cases} \tag{66}$$

and the contours of density $\Phi^* = A$ = constant, corresponding to various fixed values of the product $\omega^* \sin \theta_\infty$, are straight lines parallel to the direction of normal incidence ($\theta_\infty = \theta = 0°$) over both ω^*, θ_∞- and ω^*, θ-space. The breaking constraint (63) indicates the regions of the incident ω^*, θ_∞-space to be deleted in a progressive manner dependent on the ratio $V(x)/V_m$ and whether $dV/dx > 0$ or $dV/dx < 0$. For instance, referring to Figure 1, the spectral components in the region ABL of the incident ω^*, θ_∞-space are entirely eliminated by the time waves propagate to the section (2-2) where $V(x) = 0.5\ V_m$. Similarly, the components in the region BCKL gradually dissipate as waves advance from (2-2) to (3-3). However, beyond (3-3) where $dV/dx < 0$, wave breaking has no influence on the spectral components to the right of the line CK. For $\theta_\infty > 0$, the reflection constraint (62) suggests that, as waves propagate from (1-1) to (2-2), the part IFGH of the incident ω^*, θ_∞-space be eliminated at (2-2). Similarly, from (2-2) to (3-3), the components in the region EFIJ are reflected leaving only the part CDEJK of the incident wave space beyond (3-3) where breaking and reflection become immaterial. However, for a steady state, the reflected spectral components must be properly accounted for since they propagate back in the direction $(\pi-\theta)$ locally and modify the incident wave space. The deep water density Φ^*_∞ (=1) and the associated ω^*, θ_∞-space must, therefore, be as shown in Figure 2 by dashed lines with the region GE'J'H representing the mirror image of the part GEJH that has been progressively reflected back as waves propagated from (1-1) to (3-3). Likewise shown in Figures 3 through 5 are the transformed densities over their respective local ω^*, θ-spaces at any point along the lines (2-2), (3-3) and (4-4) of Figure 1, respectively.

In Figure 3, the region FE'J'I represents those components reflected back in between (2-2) and (3-3). Finally, Figure 6 illustrates the spectral density and the associated wave space at any point on and beyond the line (5-5) where $V(x) = 0$. The spectral magnitudes (=1) and the wave space in this figure are, therefore, exactly the same as the CDEJK part of Figure 2.

Example 2: Current Interactions in Shallow Water

By virtue of the definitions (55) through (57), we may rewrite the dispersion relation (27) as

$$\tanh k^*h^* = \frac{(\omega^*)^2[1 - \frac{V(x)}{V_m}\omega^* \sin\theta_\infty]^2}{k^*} \tag{67}$$

Under the shallow water condition

$$h^*(\omega^*)^2\,[1 - \frac{V(x)}{V_m}\omega^* \sin\theta_\infty]^2 \leq \pi/10 \tag{68}$$

we find [see, e.g., Longuet-Higgins, 1956]

$$\tanh k^*h^* \simeq \omega^*(h^*)^{1/2}[1 - \frac{V(x)}{V_m}\omega^* \sin\theta_\infty] \tag{69}$$

and

$$\frac{\partial}{\partial k^*}(\tanh k^*h^*) \simeq 2\,\omega^*(h^*)^{1/2}[1 - \frac{V(x)}{V_m}\omega^* \sin\theta_\infty] \tag{70}$$

On the basis of these results, it follows that

$$C' \simeq C_G' \simeq V_m (h^*)^{1/2} \tag{71}$$

and (32), (38), (40) and (36) become, respectively

$$\sin\theta \simeq \omega^* (h^*)^{1/2} [1 - \frac{V(x)}{V_m} \omega^* \sin\theta_\infty]^{-1} \sin\theta_\infty \tag{72}$$

$$\frac{V(x)}{V_m} \omega^* \sin\theta_\infty \leq [1 + (h^*)^{1/2}]^{-1} \quad , \quad \theta_\infty > 0 \tag{73}$$

$$-\frac{V(x)}{V_m} \omega^* \sin\theta_\infty < \frac{n}{1-n} \simeq \infty \quad , \quad \theta_\infty < 0 \tag{74}$$

$$\Phi^*(\omega^*, \theta) / \Phi_\infty^*(\omega^*, \theta_\infty) = A \tag{75}$$

where

$$A \simeq [1 - \frac{V(x)}{V_m} \omega^* \sin\theta_\infty]^3 [2h^* (\omega^*)^2]^{-1} \tag{76}$$

As a specific example here, consider a current of the form

$$V(x) = \begin{cases} V_m & ; \quad x_1 \leq x \leq x_2 \\ 0 & ; \quad \text{otherwise} \end{cases} \tag{77}$$

as schematically illustrated in Figure 7, together with the shallow water depth profile. We note that the breaking constraint (74) is redundant in this case. That is to say, no component with finite ω^* in the local ω^*, θ_o-space just before the current [see Figure 9] will ever attain a breaking condition on

account of the excessive depth refraction which progressively distorts and focuses the incident wave space to the direction of normal incidence by the time waves encounter the current field in shallow water. Provided that $< \partial h^*/\partial x \gtrsim < 0$, as assumed here, the lowest upper bound of the reflection constraint is realized at $x = x_1$ where $h^* = 0.002$. Hence, at this point the components in the DEF region of ω^*, θ_∞-space are totally reflected. These are, therefore, propagated back and superimposed on the incident wave field. In this manner, the deep-water wave space and the spectral magnitudes become as shown in Figure 8 by the dashed line boundary in which $\Phi_\infty^* = 1$ and the region $D'F'E'$ corresponds to the reflected image of that bounded by DFE. Presented in the remaining Figures 9 through 12 are the local spectral contours and wave-spaces corresponding to any point at $x = x_1^-$ (just before current), $x = x_1^+$ (right after the initial interaction), $x = x_2^-$ (just before waves exit) and $x = x_2^+$ (right after exit), respectively.

CONCLUDING REMARKS

The mean-square spectral distribution over a wave number space or a polar frequency-direction space constitutes a concise characterization for incoherent random gravity waves. The spatial transformation of this distribution by refraction due to currents and underwater topography is, therefore, of basic interest and practical importance. In the preceding, the solution to this transformation has been given for waves crossing a steady nonuniform shear current field in which variations in the surface velocity and depth-profile are unidirectional in the same sense. Various nonlinear mechanisms, dissipation and generation effects such as wave-wave, wave-wind interactions, friction, percolation,

etc. have been neglected. Some of these, e.g., friction and nonlinear wave-wave interactions, may very well be of secondary importance as suggested by previous studies [see, e.g., Munk and Traylor, 1947; Huang et.al., 1972] in comparison with the dramatic influence of currents and underwater topography on waves. Hopefully, this has been illustrated here by a few idealized examples.

ACKNOWLEDGMENTS

Financial support for this work was provided by the Geography Programs of the Office of Naval Research under contract no. N0014-76-C-0412 with the University of Delaware. The authors gratefully acknowledge helpful comments by R. G. Dean.

REFERENCES

Arthur, R. S., Refraction of shallow water waves: the combined effect of currents and underwater topography, Trans. AGU, 31(4), 549-552, 1950.

Bretherton, F. P. and Garrett, C. J. R., Wavetrains in inhomogeneous moving media, Proc. Roy. Soc., A, 302, 529-554, 1968.

Collins, J. I., Prediction of shallow-water spectra, J. Geophys. Res., 77, (15), 2693-2707, 1972.

Dalrymple, R. A., A finite amplitude wave on a linear shear current, J. Geophys. Res., 79 (30), 4498-4504, 1974a.

Dalrymple, R. A., Water waves on a bilinear shear current, Proc. 14th Coastal Engineering Conf., 1 (36), 626-641, 1974b.

Dalrymple, R. A. and Dean, R. G., Waves of maximum height on uniform currents, J. Waterways, Harbors and Coastal Eng., Amer. Soc. Civil Eng., WW3, 259-268, 1975.

Hasselmann, K., Weak-interaction theory of ocean waves, Basic Developments in Fluid Dynamics, ed. by M. Holt, 2, 117-182, Academic Press, 1968.

Huang, N. E., Chen, D. T., Tung, C. C. and Smith, J. R., Interactions between steady nonuniform currents and gravity waves with application for current measurements, J. Phys. Oceanography, 2, 420-431, 1972.

Johnson, J. W., The refraction of surface waves by currents, Trans. AGU, 28 (6), 867-874, 1947.

Karlsson, T., Refraction of continuous wave spectra, J. Waterways, Harbors and Coastal Eng., Amer. Soc. Civil Eng., WW4, 437-448, 1969.

Kenyon, K. E., Wave refraction in ocean currents, Deep-Sea Res., 18, 1023-1034, 1971.

Krasitskiy, V. P., Toward a theory of transformation of the spectrum on refraction of wind waves, Atmospheric and Oceanic Physics, 10(1), 72-82, 1974.

Landau, L. D. and Lifshitz, E. M., Fluid Mechanics, Pergamon Press, London, pp. 536, 1959.

Lighthill, M. J., Group velocity, J. Inst. Maths. Applics., 1, 1-28, 1964.

Longuet-Higgins, M. S., The refraction of sea waves in shallow water, J. Fluid Mech., 1, 163-176, 1956.

Longuet-Higgins, M. S. and Stewart, R. W., The changes in amplitude of short gravity waves on steady nonuniform currents, J. Fluid Mech., 10, 529-549, 1961.

Longuet-Higgins, M. S., On the transformation of a continuous spectrum by refraction, Proc. Cambridge Phil. Soc., 53, 226-229, 1957.

Longuet-Higgins, M. S. and Stewart, R. W., Radiation stress and mass transport in gravity waves, J. Fluid Mech., 13, 481-504, 1962.

Longuet-Higgins, M. S., Recent progress in the study of longshore currents, Waves on Beaches, edited by R. Meyer, 203-248, Academic Press, New York, 1972.

Munk, W. H. and Traylor, M. A., Refraction of ocean waves: a process linking underwater topography to beach erosion, J. Geology, 55 (1), 1-25, 1947.

Noda, E. K., Sonu, C. J., Rupert, V. C. and Collins, J. I., Nearshore circulation under sea breeze conditions and wave current interaction in the surf zone, Tetra Tech, Inc., Rep. TETRAT-P-72-149-4, pp. 1-216, Pasadena, Calif., 1974.

Peregrine, D. H., Interaction of water waves with currents, Advances in Appl. Mech., 16, in press, 1975.

Phillips, O. M., Dynamics of the Upper Ocean, pp. 1-261, Cambridge University Press, London, 1966.

Skovgaard, O., Jonsson, I. G., and Bertelsen, J. A., Computation of wave heights due to refraction and friction, J. Waterways, Harbors and Coastal Eng., Amer. Soc. Civil Eng., WW1, 15-32, 1975.

Tung, C. C. and Huang, N. E., Combined effects of current and waves on fluid force, Ocean Eng., 2, 183-193, Pergamon Press, 1973.

Ursell, F., Steady wave patterns on a nonuniform steady fluid flow, J. Fluid Mech., 9, 333-346, 1960.

Whitham, G. B., A note on group velocity, J. Fluid Mech., 9, 347-352, 1960.

Willebrand, J., Energy transport in a nonlinear and inhomogeneous random gravity wave field, J. Fluid Mech., 70 (1), 113-126, 1975.

LIST OF FIGURES

Figure 7 Example 2: Current Interactions in Shallow Water. Definition sketch in plan view (top) and profile.

Figure 8 Example 2: Current Interactions in Shallow Water. The steady state incident directional density Φ_∞^* (=1, within the dashed-line boundary), and various regions of the incident ω^*,θ_∞-space affected by reflection (DFE) as waves enter the shear current at $x = x_1$.

Figure 9 Example 2: Current Interactions in Shallow Water. Diagram of contours of $\Phi_o^* = A = \text{const}$ and the associated ω^*,θ_o-space at any point along the line $x = x_1^-$, showing the dramatic effect of pure depth refraction on the incident (ABCDEF) spectral components as well as on those reflected back ($D'F'E'$) from $x = x_1^+$ by the shear current.

Figure 10 Example 2: Current Interactions in Shallow Water. Contours of $\Phi^* = A = \text{const}$ and the associated ω^*,θ-space at any point on the line $x = x_1^+$, showing the combined effects of depth and current interactions ($h^* = 0.002$).

Figure 11 Example 2: Current Interactions in Shallow Water. Contours of $\Phi^* = A = \text{const}$ and the associated ω^*,θ-space at any point on the line $x = x_2^-$, showing again the combined effects of depth and current interactions just before waves leave the current field ($h^* = 0.001$).

Figure 12 Example 2: Current Interactions in Shallow Water. Contours of $\Phi_o^* = A = \text{const}$ and the associated ω^*,θ_o-space at any point on the line $x = x_2^+$, showing the effect of pure depth refraction right after waves cross the current ($h^* = 0.001$).

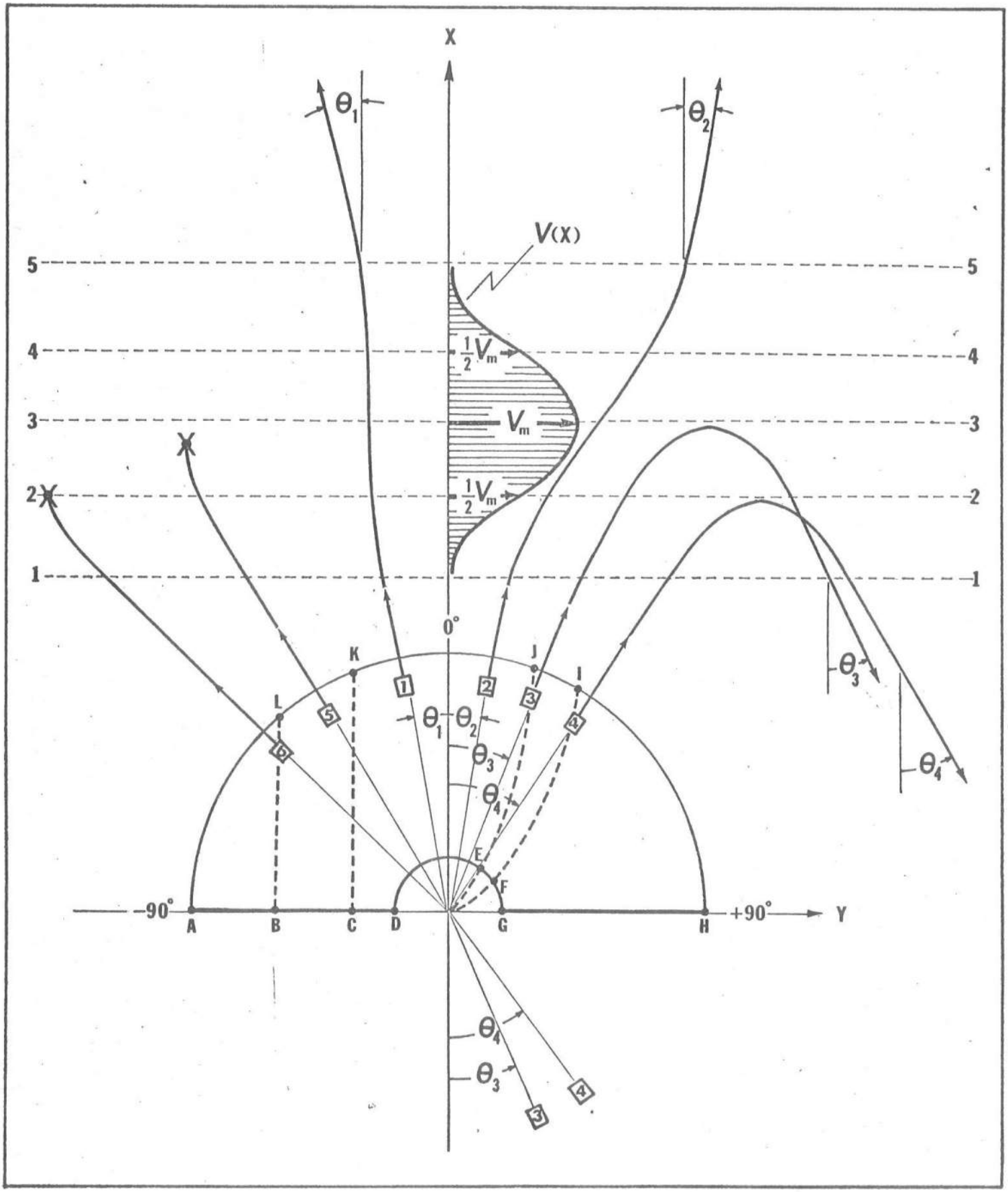

Figure 1 Example 1: Current Interactions in Deep Water. Definition sketch showing the qualitative effect of the shearing current on wave orthogonals for various angles of entry θ_∞.

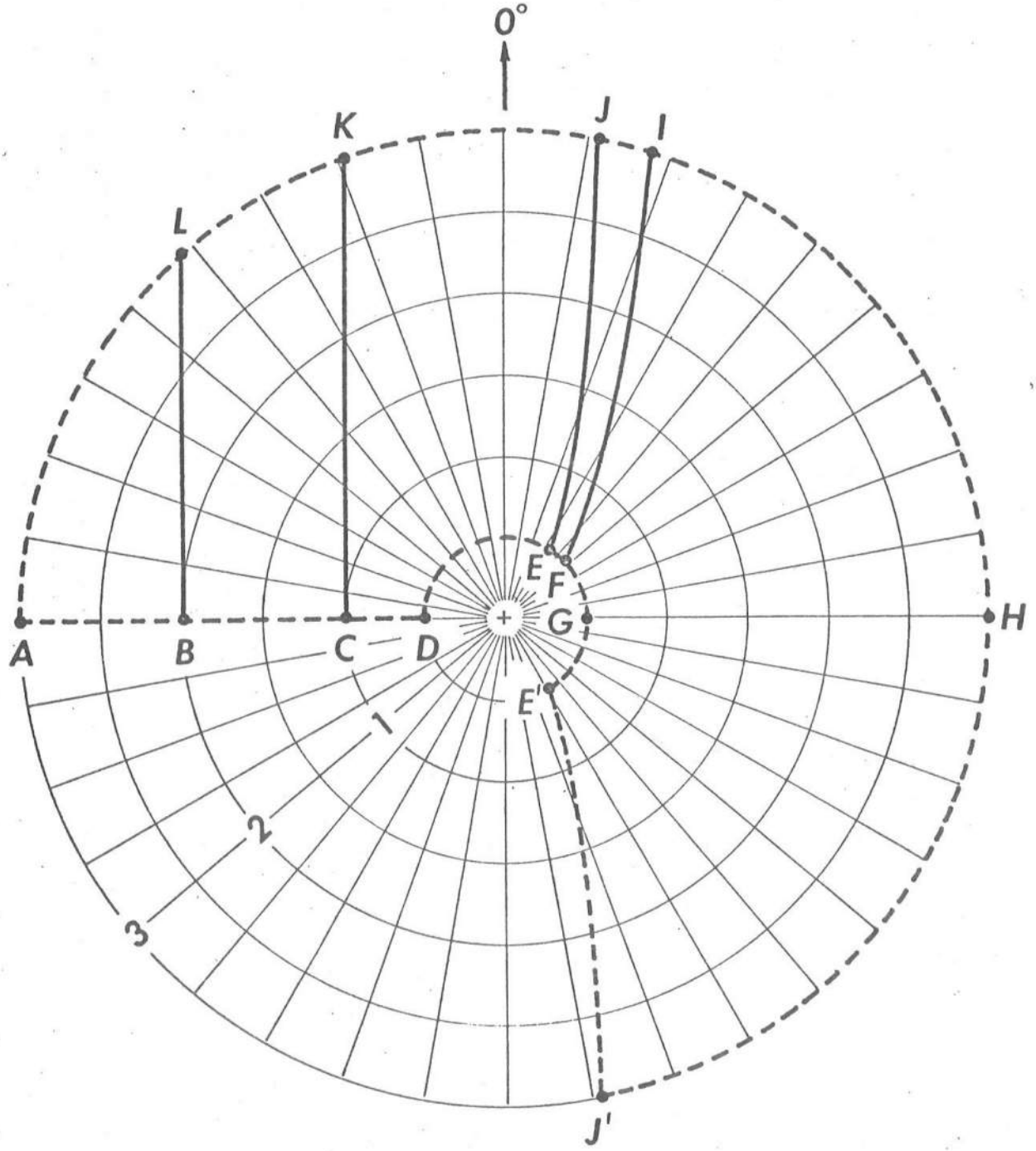

Figure 2 Example 1: Current Interactions in Deep Water. Diagram showing the steady state incident directional density Φ_∞^* (=1, within the dashed-line boundary), and various regions of the incident ω^*, θ_∞-space affected by breaking and reflection as waves cross the current.

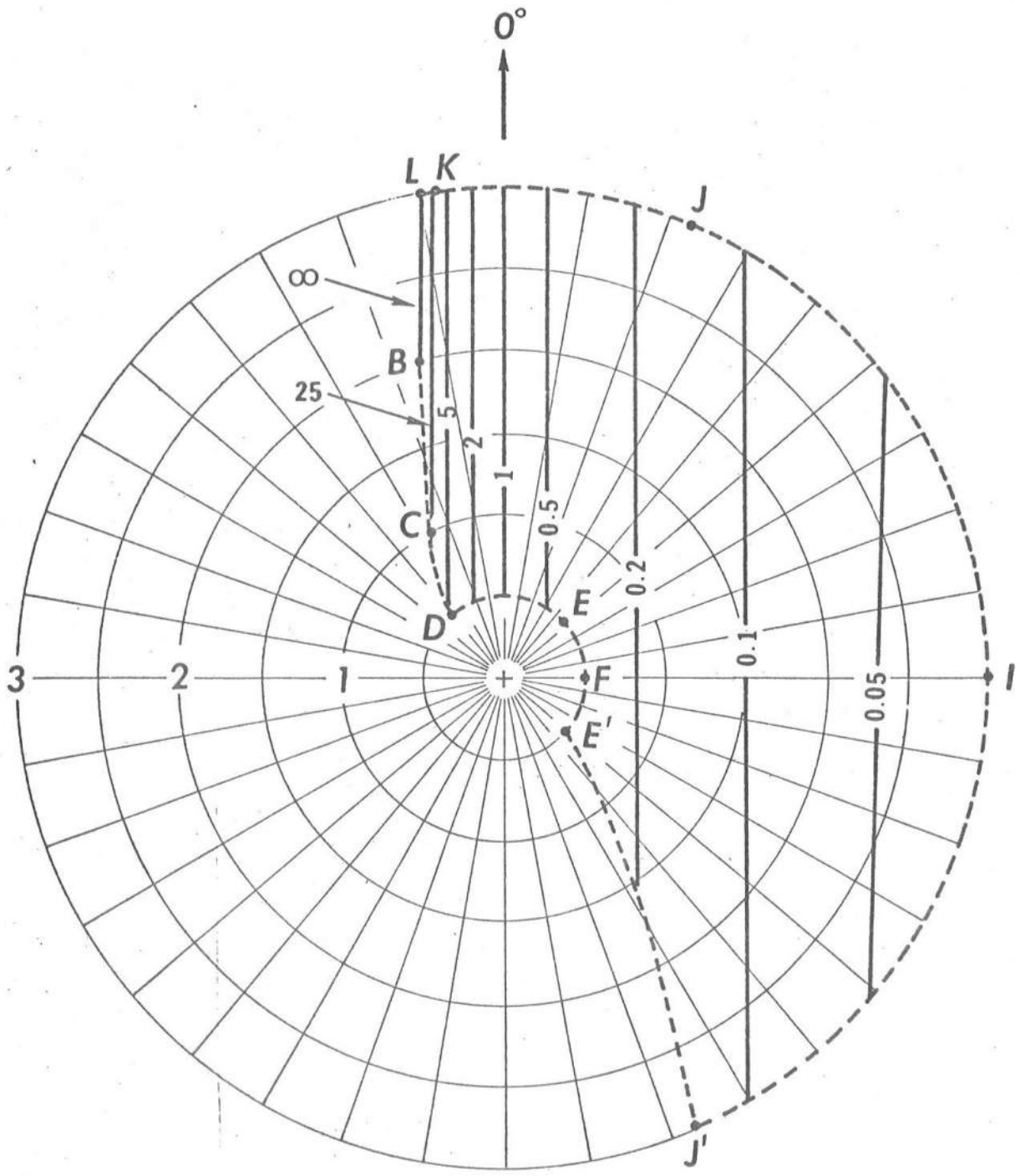

Figure 3 Example 1: Current Interactions in Deep Water. Contours of $\phi^* = A =$ const and the associated ω^*, θ-space at any point along section 2-2.

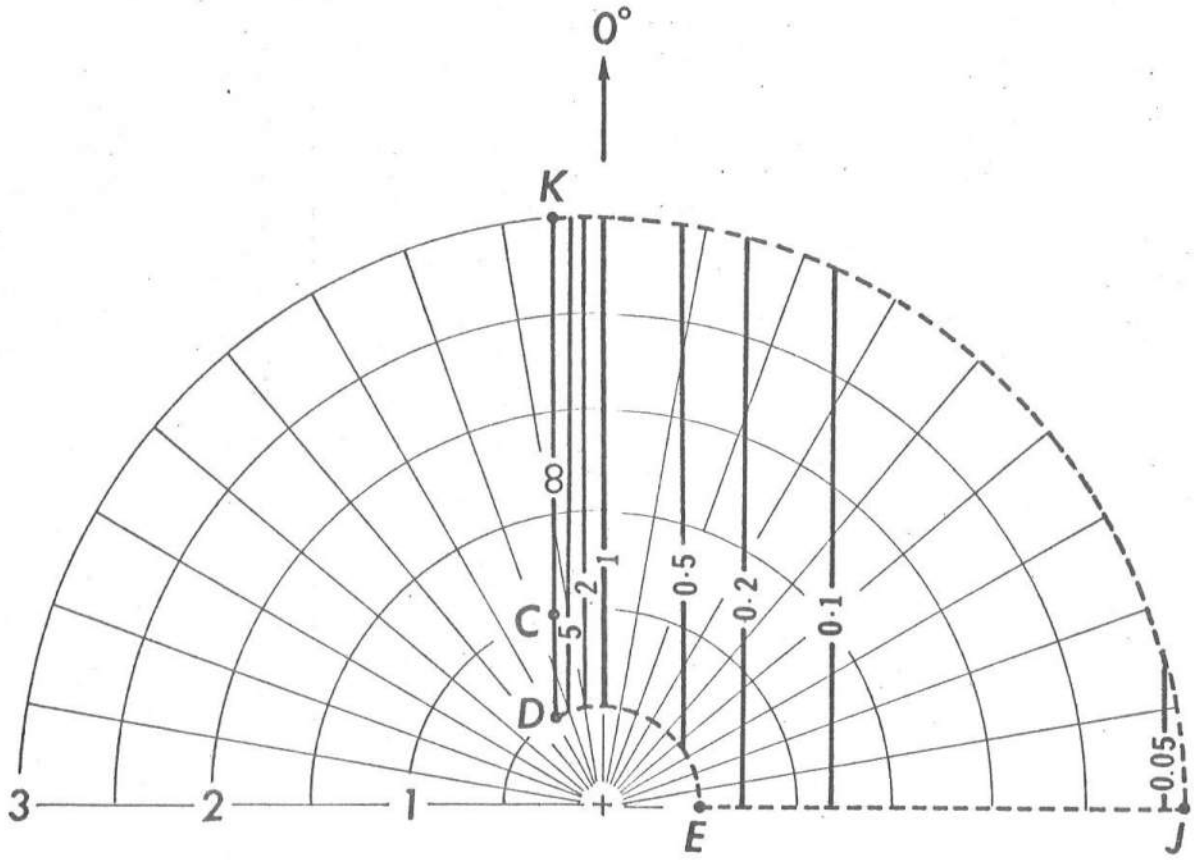

Figure 4 Example 1: Current Interactions in Deep Water. Contours of $\Phi^* = A =$ const and the associated ω^*,θ-space at any point along section 3-3.

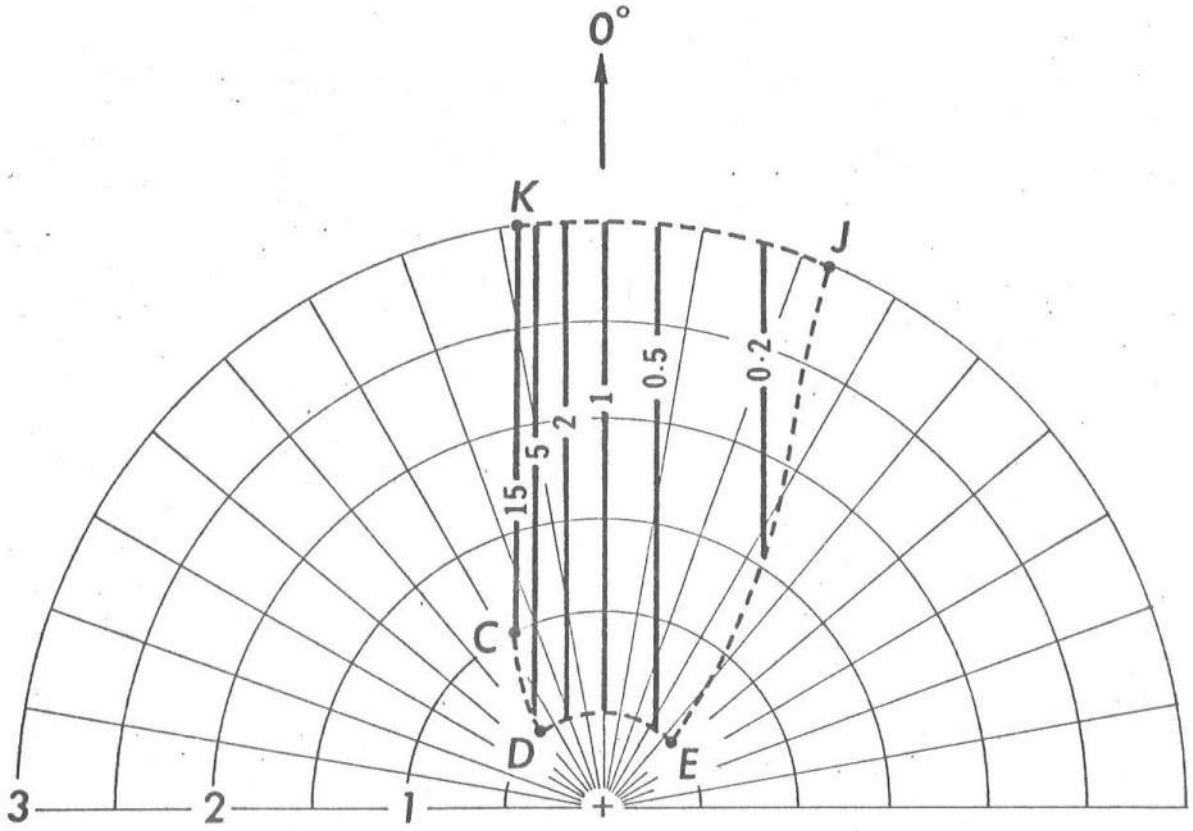

Figure 5 Example 1: Current Interactions in Deep Water. Contours of $\phi^* = A =$ const and the associated ω^*, θ-space at any point along section 4-4.

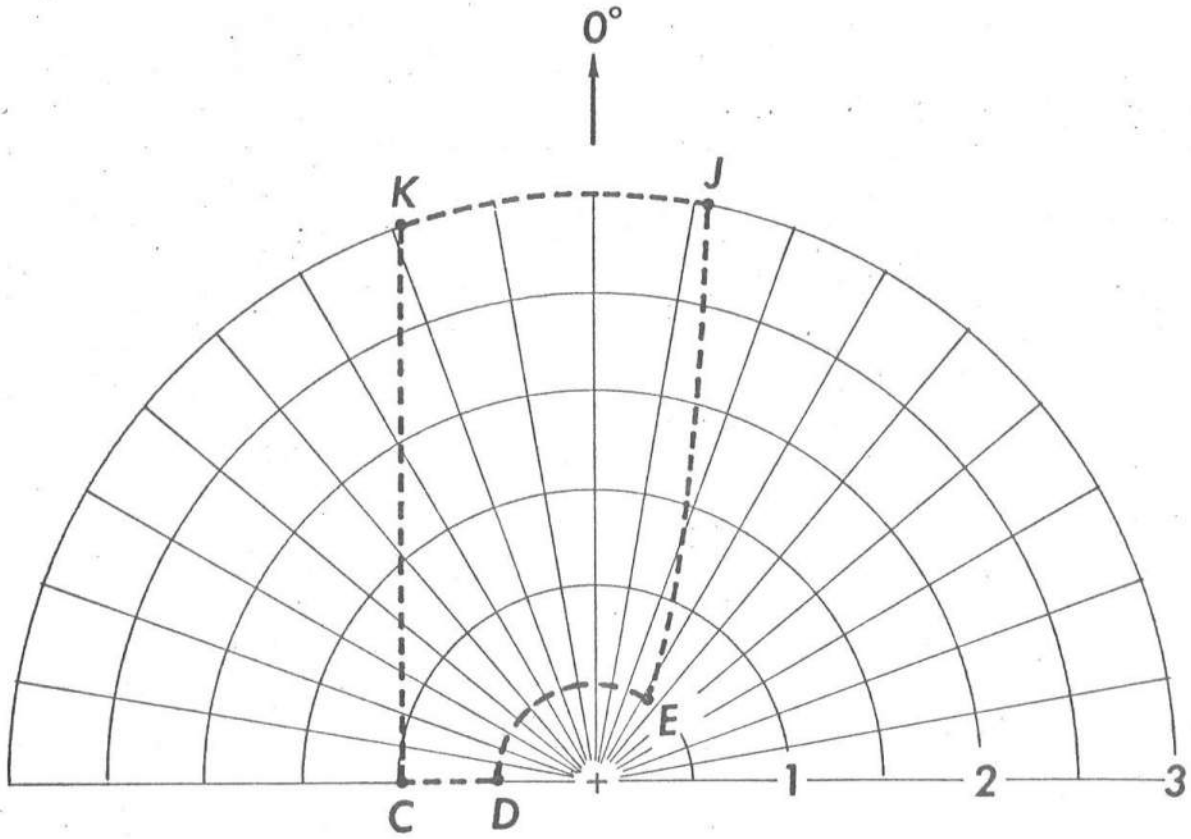

Figure 6 Example 1: Current Interactions in Deep Water. The directional spectral density $\Phi^* = \Phi_\infty^*$ (=1, within the dashed-line boundary) and the associated ω^*,θ-space (= ω^*,θ_∞) at any point on and beyond section 5-5.

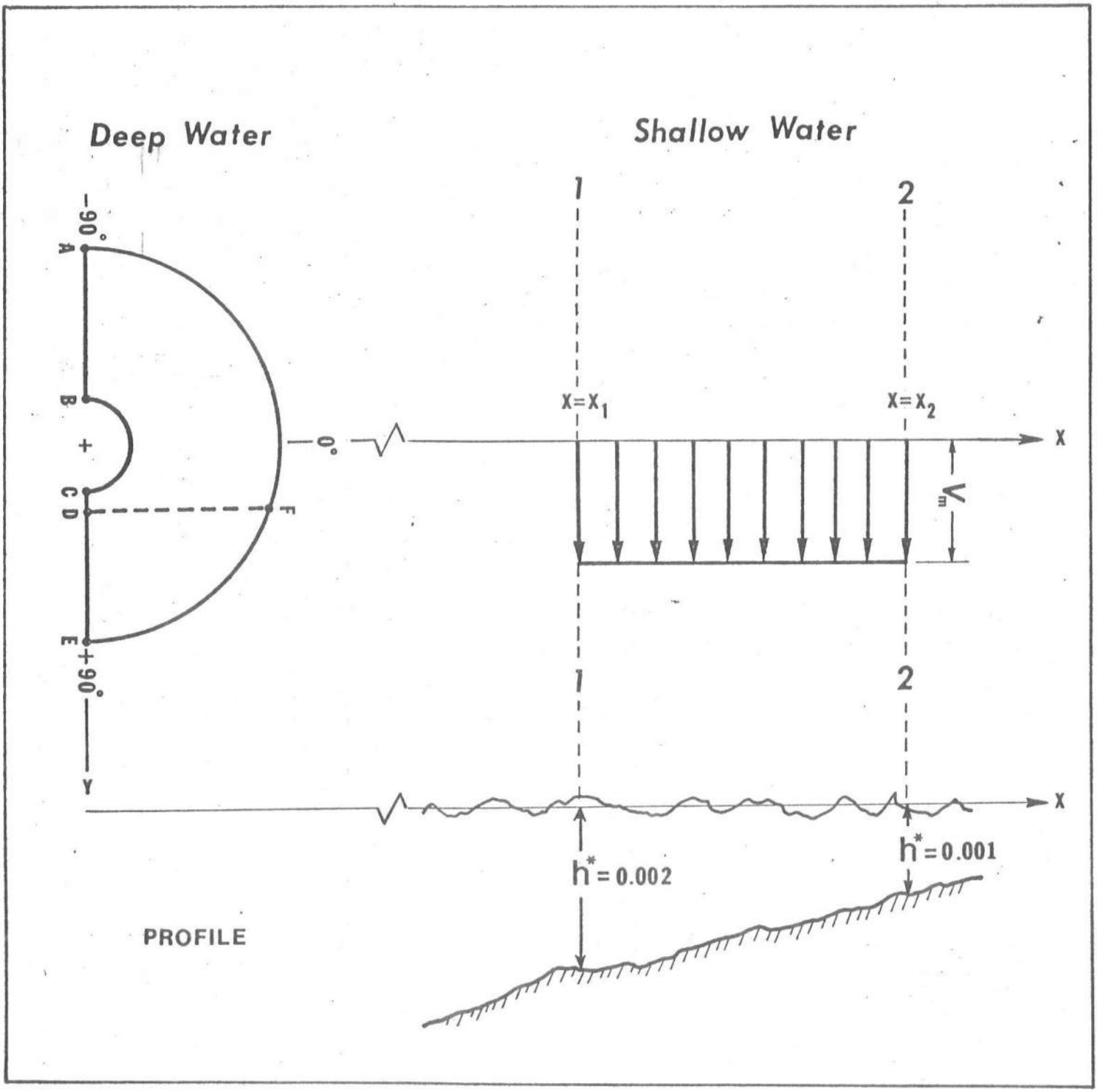

Figure 7 Example 2: Current Interactions in Shallow Water. Definition sketch in plan view (top) and profile.

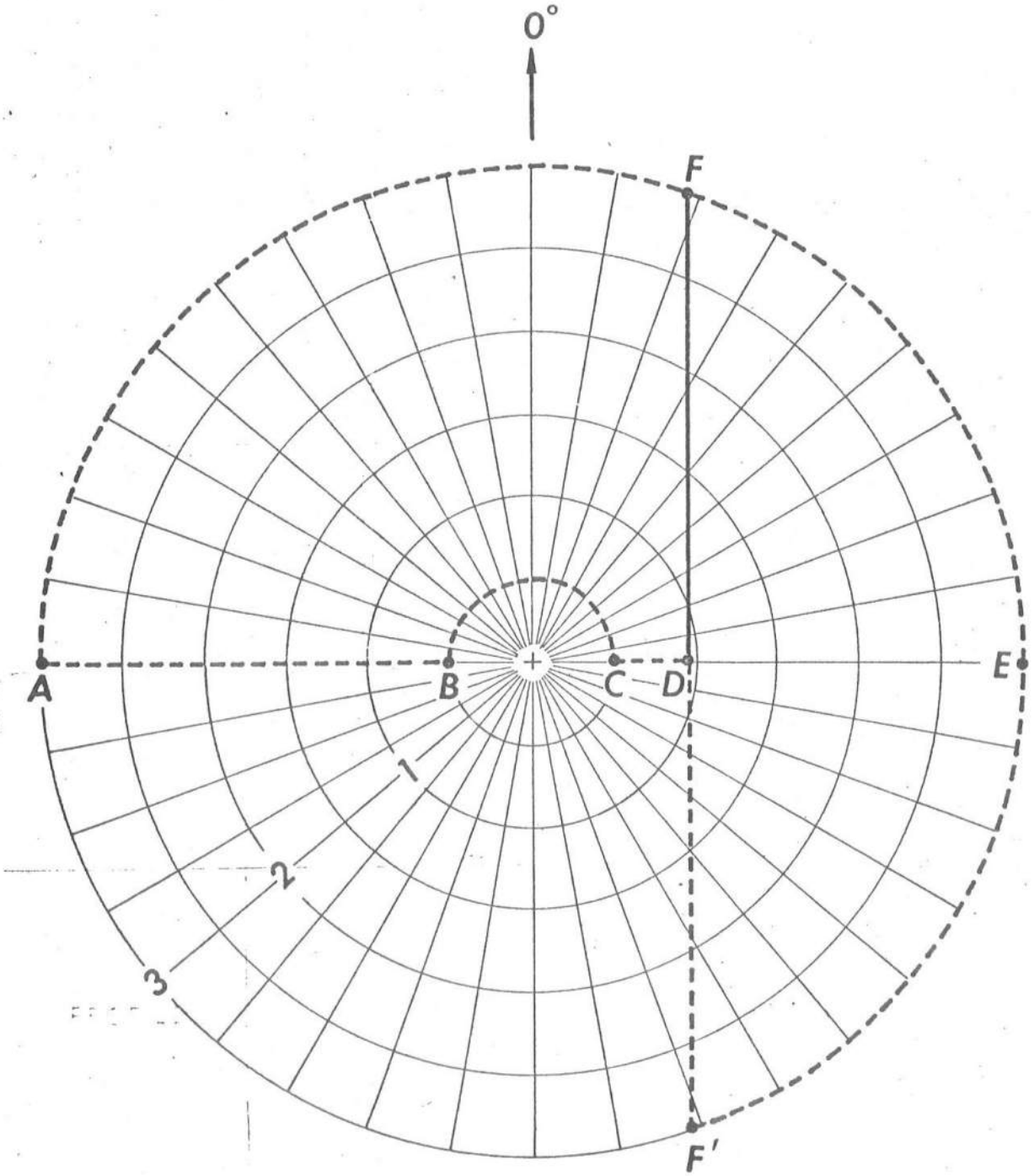

Figure 8 Example 2: Current Interactions in Shallow Water. The steady state incident directional density Φ_∞^* (=1, within the dashed-line boundary), and various regions of the incident ω^*, θ_∞-space affected by reflection (DFE) as waves enter the shear current at $x = x_1$.

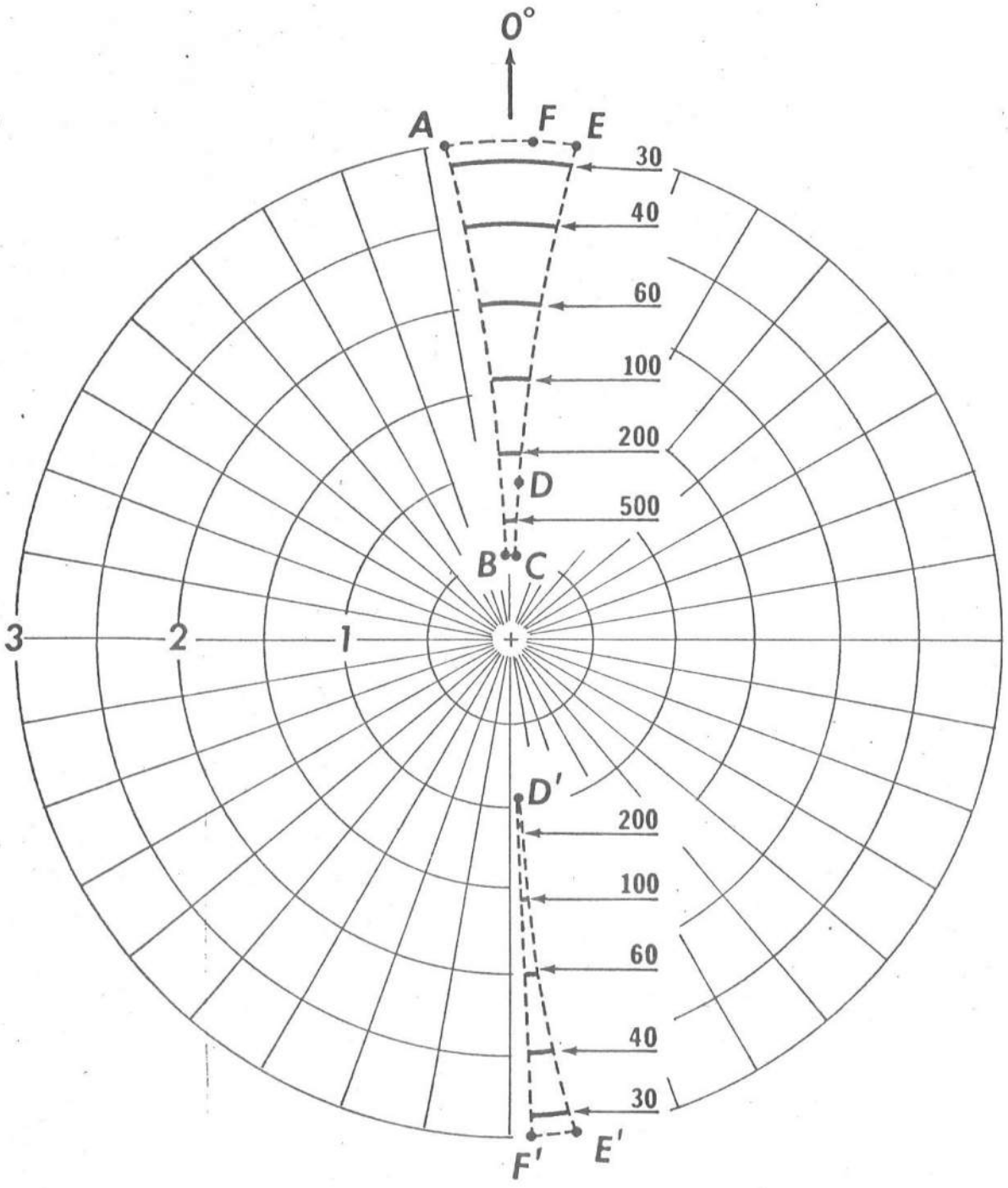

Figure 9 Example 2: Current Interactions in Shallow Water. Diagram of contours of $\Phi_o^* = A = \text{const}$ and the associated ω^*, θ_o-space at any point along the line $x = x_1^-$, showing the dramatic effect of pure depth refraction on the incident (ABCDEF) spectral components as well as on those reflected back (D'F'E') from $x = x_1^+$ by the shear current.

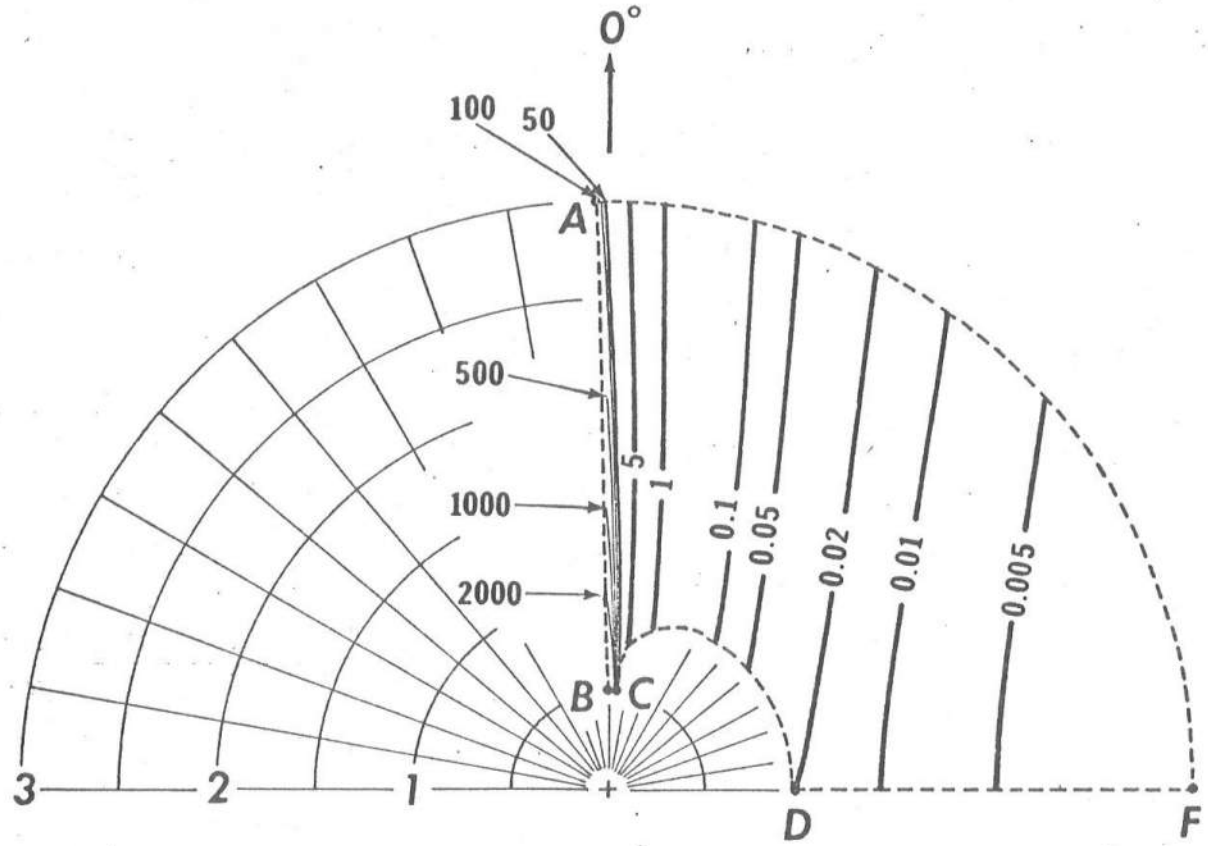

Figure 10 Example 2: Current Interactions in Shallow Water. Contours of $\phi^* = A = \text{const}$ and the associated ω^*,θ-space at any point on the line $x = x_1^+$, showing the combined effects of depth and current interactions ($h^* = 0.002$).

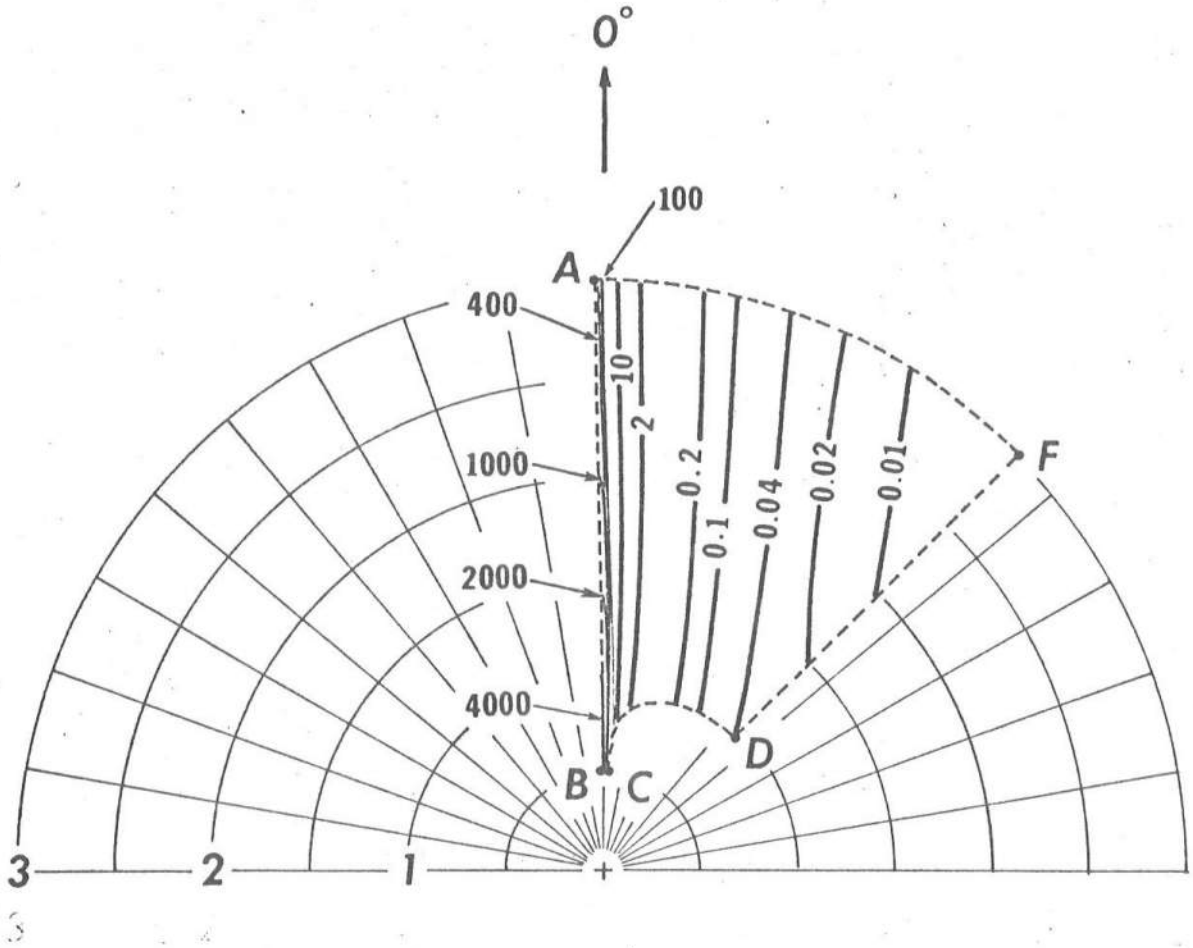

Figure 11 Example 2: Current Interactions in Shallow Water. Contours of $\phi^* = A = \text{const}$ and the associated ω^*,θ-space at any point on the line $x = x_2$, showing again the combined effects of depth and current interactions just before waves leave the current field ($h^* = 0.001$).

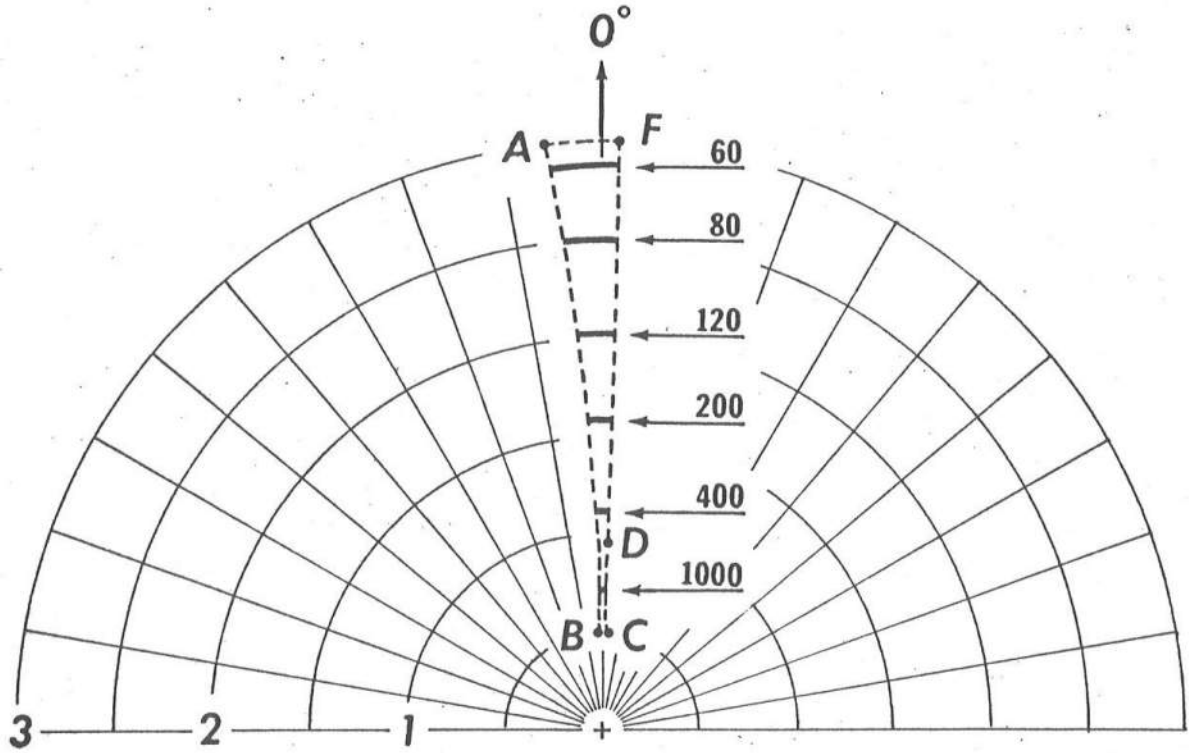

Figure 12 Example 2: Current Interactions in Shallow Water. Contours of $\Phi_o^* = A = \text{const}$ and the associated ω^*, θ_o-space at any point on the line $x = x_2^+$, showing the effect of pure depth refraction right after waves cross the current ($h^* = 0.001$).